

Hindawi Publishing Corporation
Advances in Materials Science and Engineering
Volume 2012, Article ID 180679, 6 pages
doi:10.1155/2012/180679

Research Article

Simulation of Electronic Structure of Aluminum Phosphide Nanocrystals Using Ab Initio Large Unit Cell Method

Hamad R. Jappor,¹ Zeyad Adnan Saleh,² and Mudar A. Abdulsattar³

¹Department of Physics, College of Education, University of Babylon, P.O. Box 4, Hilla, Iraq

²Department of Physics, College of Science, Al-Mustansiriyah University, P.O. Box 46010, Baghdad, Iraq

³Directorate of Materials Research, Ministry of Science and Technology, P.O. Box 8012, Baghdad, Iraq

Correspondence should be addressed to Mudar A. Abdulsattar, mudarahmed3@yahoo.com

Received 20 January 2012; Accepted 9 March 2012

Academic Editor: Markku Leskela

Copyright © 2012 Hamad R. Jappor et al. This is an open access article distributed under the Creative Commons Attribution License, which permits unrestricted use, distribution, and reproduction in any medium, provided the original work is properly cited.

Ab initio restricted Hartree-Fock method coupled with the large unit cell method is used to determine the electronic structure and physical properties of aluminum phosphide (AlP) nanocrystals between 216 and 1000 atoms with sizes ranging up to about 3 nm in diameter. Core and surface parts with different sizes are investigated. Investigated properties include total energy, cohesive energy, energy gap, valence band width, ionicity, and degeneracy of energy levels. The oxygenated (001)-(1 × 1) facet that expands with larger sizes of nanocrystals is investigated to determine the rule of the surface in nanocrystals electronic structure. Results revealed that electronic properties converge to some limit as the size of the large unit cell increases and that the 216 core atoms approaches bulk of Aluminum phosphide material in several properties. Increasing nanocrystals size also resulted in a decrease in lattice constant, increase of core cohesive energy (absolute value), increase of core energy gap, increase of core valence band width and decrease of ionicity. Valence and conduction bands are wider on the surface due to splitting and oxygen atoms. The method also shows fluctuations in the converged energy gap, valence band width and cohesive energy of core part of nanocrystals duo to shape variation.

1. Introduction

Semiconductor nanostructures have been of particular interest because confinement effects lead to large increase in the band gap (blue shift) and efficient light emission, even in Si for which coupling to light is extremely weak in the bulk crystal [1]. In the case of a pure semiconductor, the broken bonds lead to reconstruction of the surface, and in the smallest clusters, there is little resemblance to the bulk structures. On the other hand, terminating the surface by atoms such as hydrogen, which remove the dangling bonds makes the resulted cluster much more like a small, terminated piece of the bulk. Aluminum phosphide (AlP), with one of the largest direct gaps of the III-V compound semiconductors, is undoubtedly the most “exotic” and least studied [2]. At normal conditions, AlP crystallizes in the zinc blende (zb) structure. However, in recent years, it attracted special attention to its incorporation in the AlAs/AlP- and GaP/AlP-based heterostructures. AlP

is a subject of extensive theoretical studies ranging from the semiempirical to the first principles methods [3], within the density functional theory (DFT) framework using both pseudopotential [4], and all-electron approaches. For the bulk properties of AlP, theoretical calculations based on the Hartree-Fock [5], and potential model [6] have obtained a very good description of its structural and electronic properties. Recently, Annane et al. [7] investigated the structural and electronic properties of AlAs and AlP compounds using the full potential linearized augmented plane wave plus local orbitals method based on density functional theory.

The present work addresses large nanocrystals that have the size range of 216–1000 total atoms. These atoms are divided between core and surface. The present lower limit (of atoms) is chosen since it provides the first occurrence of idle core part (nearly ideal zincblende structure) that is far from surface reconstruction by more than three surface layers. To the best of our knowledge, no theoretical investigations of

cubic zb AlP nanocrystals have appeared in the literature up to the present date.

In the present work, we study the electronic structure and physical properties of AlP nanocrystals core and surface part with different sizes by using an ab initio restricted Hartree-Fock (RHF) method coupled with large unit cell method (LUC-RHF). LUC method was formulated and used before for several kinds of bulk materials including diamond and zinc blend (zb) structured materials [8–11].

2. Computational Details

Ab initio self-consistent Hartree-Fock (RHF) is used to obtain Aluminum phosphide nanocrystal molecular orbitals. Correlation corrections are neglected in the present calculations relying on Koopmans theorem [12]. This theorem states that comparisons of Hartree-Fock closed-shell results (which is the case in the present work) with experimental values suggest that in many cases the energetic corrections due to relaxation effects nearly cancel the corrections due to electron correlation. Simple STO-3G basis [13, 14] is used in the present work to reach higher number of core and surface atoms.

This method uses ($\mathbf{k} = 0$) approximation, that is, one point in the wave vector space. The LUC method is one kind of supercell methods with the above $\mathbf{k} = 0$ restriction. In this method, instead of adding more \mathbf{k} points, the single central cell is expanded to contain more atoms, which are now called core atoms in the present work. The LUC method was first suggested and applied to covalent semiconductors in the 1970s [10, 15]. The method was found suitable for nanocrystal calculations because the $\mathbf{k} = 0$ approximation retains only one central cluster of atoms surrounded by other atoms to passivate the outer dangling bonds [16]. The method is used to simulate parts of specific symmetry in the nanocrystal (core and surface) in the same way it is used for bulk materials.

We used 3D PBC (Periodic Boundary Condition) method in GUSSIAN 03 code [17] to calculate ab initio restricted Hartree-Fock electronic structure of AlP nanocrystals internal core. The 2D PBC calculations are used to simulate oxygenated (001)-(1 × 1) surface. In the present work, we divided the work into two parts, core and surface parts, which is the traditional method used in microscopic-size solid-state calculations. In LUC core part only the lattice constant is optimized, at the surface part all bond lengths and lattice constant still need to be optimized because of surface reconstruction. The (001) chosen surfaces are terminated by oxygen atoms to passivated dangling bonds. The width of surface part is set to one conventional lattice that is deduced from AlP surface bonds calculations. The oxygenated (001)-(1 × 1) AlP surface in the oxygen double bonding configuration is investigated to obtain the total electronic structure of the AlP nanocrystal with (001)-(1 × 1) facets. The oxygenated (001)-(1 × 1) AlP surface is chosen since it is one of the least reconstructed surfaces. Unlike the core part, the bond lengths and lattice constant are not unique and a variation of geometrical parameters is needed. Normally surface

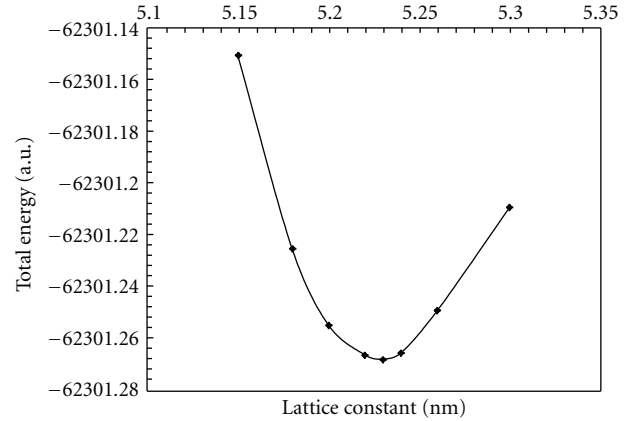


FIGURE 1: Total energy of 216 atoms aluminum phosphide core LUC as a function of lattice constant.

effects do not penetrate more than four layers (one lattice constant) from the crystal surface [18]. On the other hand, short-range sp^3 bonds do not require more than fourth neighbor's interaction range to conduct electronic structure calculations successfully using molecular orbital methods [16]. The upper two identical conditions are applied in the present calculations.

Two kinds of core LUCs are investigated, namely, cubic and parallelepiped cells. The cubic cells are multiples of zb structure Bravais unit cells, while the parallelepiped cells are multiples of primitive zb structure unit cells [18]. Cubic core cells include 8, 64, and 216 atoms. Parallelepiped cells include 16, 54, 128, and 250 atoms.

3. Calculations and Results

In this section, we present the calculated band structures of aluminum phosphide nanocrystals. Figure 1 shows the total energy for AlP nanocrystal as a function of lattice constant for 216 core atoms, from which we obtained the equilibrium lattice constant. Figure 2 shows the variation of the lattice constant of aluminum phosphide nanocrystals core as a function of number of core atoms. This figure is obtained after minimizing the energy lattice curve of every investigated number of core atoms. From this figure, we see that the lattice constant for the core part of the crystal decrease with increasing number of atoms. The converged lattice length for a high number of core atoms (0.523 nm) is in good agreement with the experimentally reported value (0.545 nm) for bulk [19, 20].

The bulk modulus B can be obtained using the equation of state of Murnghan [21]. Bulk modulus of AlP nanocrystal as a function of number of atoms in the core is shown in Figure 3. This figure shows that the bulk modulus increases with the number of atoms in the core. We note that the bulk modulus for AlP nanocrystal of 97 GPa is in reasonable agreement with the experimental value of 86 [19] of the bulk taking into consideration that Hartree-Fock theory always overestimates bulk modulus values [8].

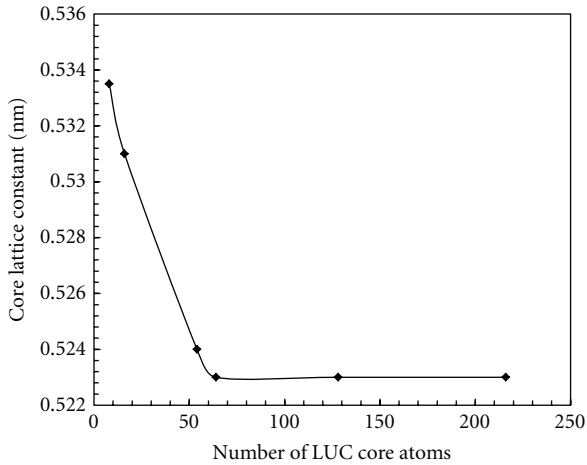


FIGURE 2: Energetically optimized zb-AIP core lattice constant as a function of the number of atoms in the core.

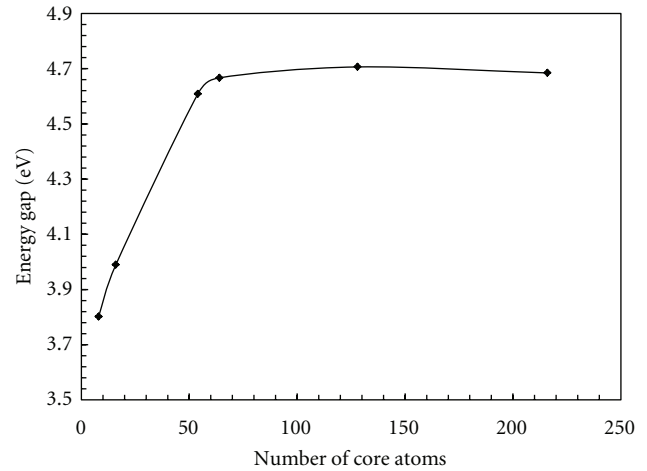


FIGURE 4: Energy gap of the core part of zb-AIP nanocrystals as a function of the number of core atoms.

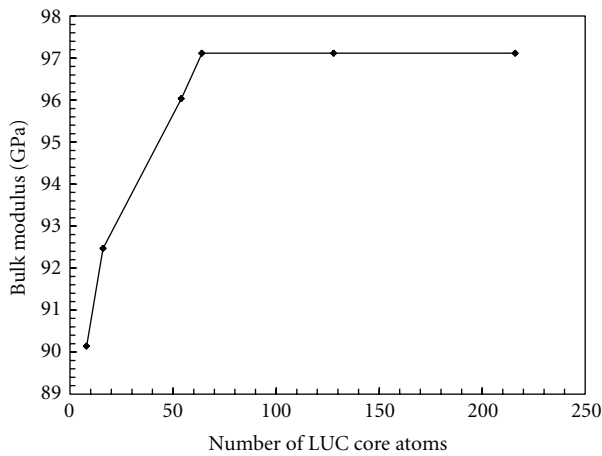


FIGURE 3: Bulk modulus as a function of the number of core atoms.

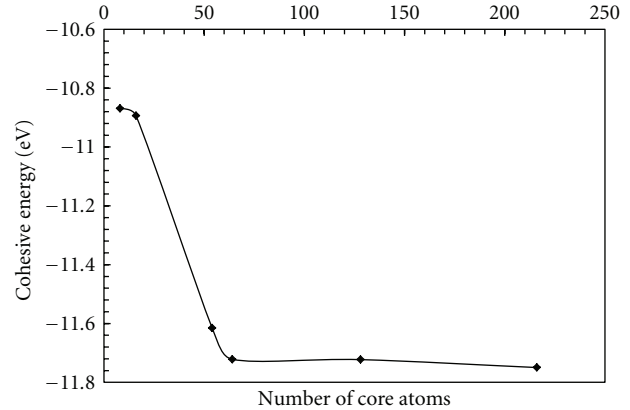


FIGURE 5: Cohesive energy of the core part of zb-AIP nanocrystals as a function of the number of core atoms.

AIP has an indirect minimum gap between highest occupied molecular orbital (HOMO) and lowest unoccupied molecular orbital (LUMO) with the CBM at X point of the Brillouin zone [22]. Figure 4 shows the energy gap of the core part of the investigated nanocrystals against the number of core atoms. The increase of the energy gap in the first part of the considered range is not a violation of the quantum confinement theory since the energy gap is controlled by the surface part gap [23, 24], which is much smaller gap than the core part. All energies converge quickly for the nanocrystals with more than 64 core atoms with a very wide energy gap variation range approximately (3.80 eV to 4.69 eV), which is higher than the experimentally reported energy gap (2.45–2.5 eV) for bulk zb-AIP [25, 26] but within the trends of nanocrystals blue shift [23, 24, 27, 28]. The relation between the cohesive energy and the number of atoms is shown in Figure 5. A reasonable agreement for the cohesive energy with experimental data (8.34 eV) [29] and other calculations [20, 30] of the bulk value (8.27–9.73 eV). Figure 5 shows that the cohesive energy decreases with increasing number of

atoms with small fluctuation after (–11.721 eV) for the cell which contains 64 core atoms.

In the present work, we calculated valence bandwidth which is the difference between HOMO and LUMO levels. The valence bandwidth as a function of number of atoms for AIP nanocrystal core part is shown in Figure 6. One can see from the figure that this band generally increases with increasing number of atoms and becomes nearly stable at the 64 core atoms.

The ionicity charge is calculated as a function of number of core atoms. Figure 7 shows that smaller nanocrystals are more ionic than larger ones.

Figure 8 shows the variation of highest occupied molecular orbital energy (HOMO) and lowest unoccupied molecular orbital energy (LUMO) as the core of nanocrystals grows up in size and changes its shape. This curve fluctuates strongly because of the change in size and shape that produces different surfaces with different properties. HOMO and LUMO variation shows that not all quantities have definite convergence behaviour similar to the upper investigated quantities.

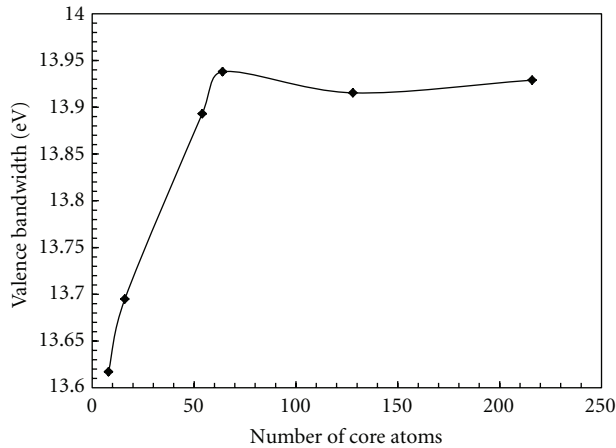


FIGURE 6: Valence bandwidth of the core part of zb-AlP nanocrystals as a function of core atoms.

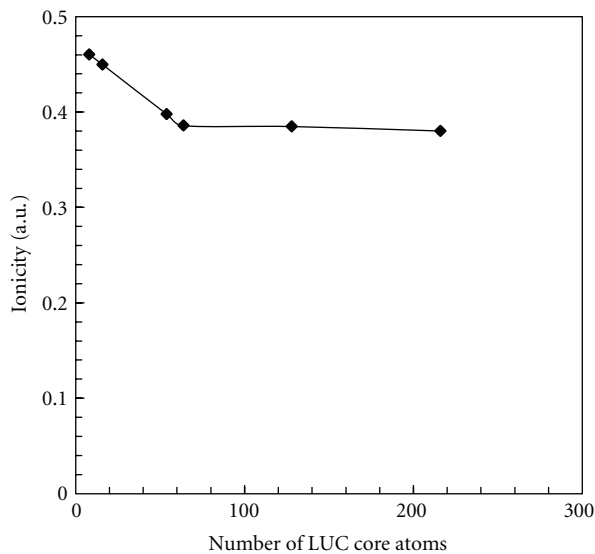


FIGURE 7: Ionicity of the core part of zb-AlP nanocrystals as a function of the number of core atoms.

HOMO and LUMO energy levels plotted in Figure 8 show fluctuating behaviour that continues indefinitely. A negative sign to the approximate ionization potential and affinity, respectively, [31] relates HOMO and LUMO levels. As nanocrystals grow up in size they develop different shapes and surfaces. Each of the developed surfaces has different properties such as the upper mentioned ionization potential and affinity or HOMO and LUMO energy levels. Therefore, these fluctuations start at the nanoscale, continue to the micro-, and bulk scale. A similar behaviour is observed for BP and SiGe nanocrystals [27, 32].

The degeneracy of energy level states for AlP nanocrystal as a function of energy levels for the lowest energy lattice constant is calculated for core and surface parts. Figure 9 shows the degeneracy of states for 8 atoms of core part. Due to high symmetry, the number of degenerate states is high in the core part. The highest number of degenerate states in the valence band is between 6 for the 8 atom cores and 30 for the

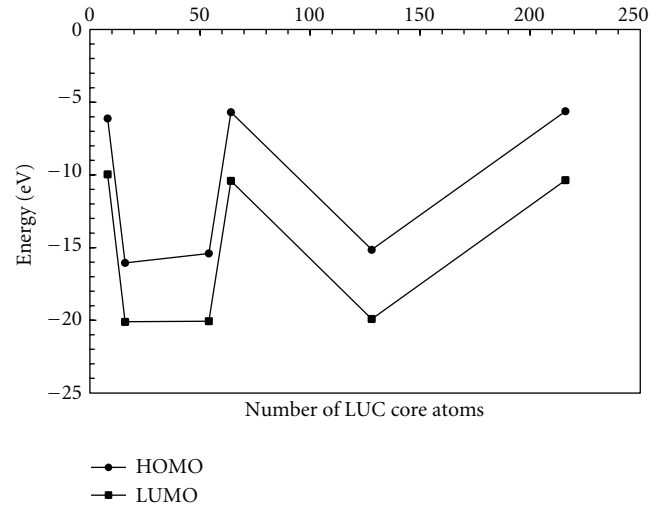


FIGURE 8: HOMO and LUMO energies that correspond to different core sizes of AlP nanocrystals.

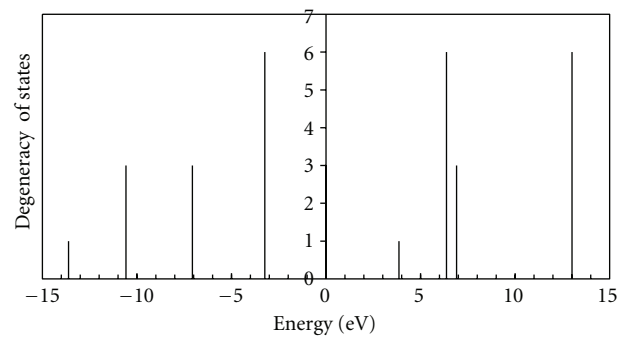


FIGURE 9: Degeneracy of states of 8-atom core part of zb-AlP nanocrystal as a function of level energy. The HOMO level is taken as the reference level.

216 atom cores. A similar behaviour is observed for diamond nanocrystals *ab initio* large unit cell calculations [33] and SiC nanocrystals [34].

To investigate nanocrystals surface electronic structure, it is natural to assume that larger nanocrystals have larger surfaces. Three oxygenated oxygen terminated (001)-(1 × 1) zb-AlP surface stoichiometry slabs are investigated, namely, Al₈O₄P₈, Al₃₂O₁₆P₃₂, and Al₇₂O₃₆P₅₄ with three surface areas of a², 4a², and 9a², respectively, where (a) is the lattice constant.

The results of the oxygenated (001)-(1 × 1) surface for the lattice constant and the energy gap for the three different areas are shown in Figures 10 and 11, respectively.

The average lattice constants of the three investigated stoichiometries are less than the corresponding core parts, but they follow the same decreasing order. On the other hand, the energy gap of (001)-(1 × 1) oxidized surface shows much smaller gap than that of the core part.

The oxygenated (001)-(1 × 1) surface slab calculations of the nanocrystal converge to approximately the same lattice constant value of the core (0.5195 nm). This good matching

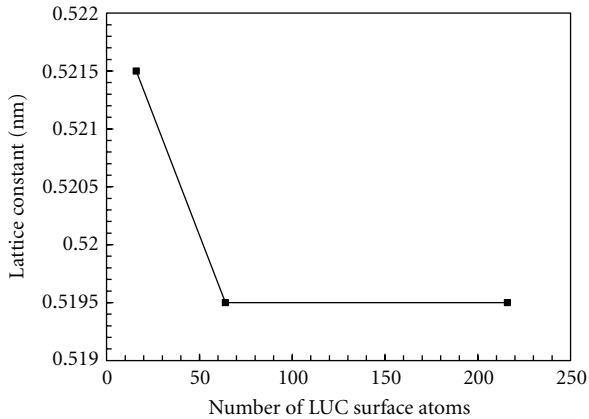


FIGURE 10: Lattice constant variation as a function of nanocrystal oxygenated (001)-(1 × 1) surface face.

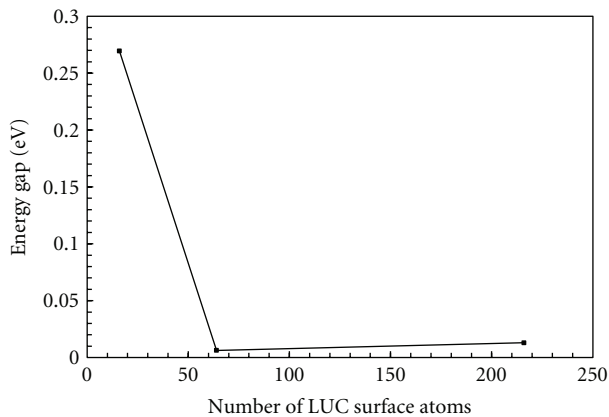


FIGURE 11: Energy gap of ALP nanocrystals oxygenated face as a function of surface area of nanocrystals facet.

between surface and core lattice constants shows that good adhesion is expected between the two parts.

In the surface part, discontinuity of surface imposes level splitting on the degenerate energy levels. The splitting of energy levels does not only affect the number of degenerate states, but also the valence and conduction bandwidths which are wider in surface part. On the other hand, the splitting of states and additional oxygen surface states strongly affect the energy gap and considerably reduce its value.

Figure 12 represents the degeneracy of states for oxygenated (001)-(1 × 1) surface part of $\text{Al}_8\text{O}_4\text{P}_8$ stoichiometry slab nanocrystal surface. This surface has lower number of degenerate states compared with core part of Figure 9. This low degeneracy is due to broken symmetry at the surface discontinuity. The existence of oxygen atoms leads to varying the bond lengths and lattice constant. Because of splitting, energy gap is reduced (see Figure 11).

4. Conclusions

In this paper, we studied some properties of zb-ALP nanocrystals. The total energy, lattice constant, bulk modulus, cohesive energy, energy gap, valence bandwidth, ionicity,

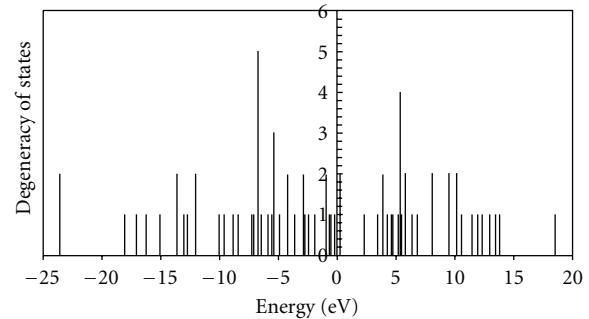


FIGURE 12: Degeneracy of states of surface part of $\text{Al}_8\text{O}_4\text{P}_8$ stoichiometry slab as a function of level energy. The HOMO level is taken as the reference level.

and degeneracy of energy levels have been calculated by the self-consistent restricted Hartree-Fock method coupled with the large unit cell method (RHF-LUC). The lattice constant and ionicity decreases with increasing size of large unit cell for core and surface parts. Cohesive energy of zb-ALP nanocrystals increases (absolute value) with the increase of number of atoms. Valence bandwidth increases with increasing size of LUC for core and surface part. Core energy gap increases with increasing size of LUC; however, surface gap decreases. The Valence bandwidth in surface part is larger than that for core part caused by the existence of oxygen atoms and surface states splitting. The degeneracy of states of core part for all sizes of LUC is larger than the degeneracy of surface part. On the other hand, (001)-(1 × 1) oxidized surface show much smaller gap and slightly larger lattice constant.

References

- [1] R. M. Martin, *Electronic Structure Basic Theory and Practical Methods*, Cambridge University Press, Cambridge, UK, 2005.
- [2] I. Vurgaftman, J. R. Meyer, and L. R. Ram-Mohan, "Band parameters for III-V compound semiconductors and their alloys," *Journal of Applied Physics*, vol. 89, no. 11, pp. 5815–5875, 2001.
- [3] A. Mujica, A. Rubio, A. Munoz, and R. Needs, "High-pressure phases of group-IV, III-V, and II-VI compounds," *Reviews of Modern Physics*, vol. 75, no. 3, pp. 863–912, 2003.
- [4] A. Mujica, P. Rodríguez-Hernández, S. Radescu, R. J. Needs, and A. Muñoz, "AIX (X = As, P, Sb) compounds under pressure," *Physica Status Solidi B*, vol. 211, no. 1, pp. 39–43, 1999.
- [5] S. Froyen and M. Cohen, "Structural properties of III-V zinc-blende semiconductors under pressure," *Physical Review B*, vol. 28, no. 6, pp. 3258–3265, 1983.
- [6] A. Jivani, H. Trivedi, P. N. Gajjar, and A. Jani, "Total energy, equation of state and bulk modulus of ALP, AlAs and AlSb semiconductors," *Pramana*, vol. 64, no. 1, pp. 153–158, 2005.
- [7] F. Annane, H. Meradji, S. Ghemid, and F. El Haj Hassan, "First principle investigation of AlAs and ALP compounds and ordered AlAs_{1-x}P_x alloys," *Computational Materials Science*, vol. 50, no. 2, pp. 274–278, 2010.
- [8] M. A. Abdulsattar and K. H. Al-Bayati, "Corrections and parametrization of semiempirical large unit cell method for covalent semiconductors," *Physical Review B*, vol. 75, no. 24, Article ID 245201, 2007.

- [9] R. A. Evarestov, M. I. Petrashen, and E. M. Ledovskaya, "The translational symmetry in the molecular models of solids," *Physica Status Solidi B*, vol. 68, no. 1, pp. 453–461, 1975.
- [10] A. Harker and F. Larkins, "A large unit cell semiempirical molecular orbital approach to the properties of solids. I. General theory," *Journal of Physics C*, vol. 12, no. 13, pp. 2487–2495, 1979.
- [11] A. Harker and F. Larkins, "A large unit cell semiempirical molecular orbital approach to the properties of solids. II. Covalent materials: diamond and silicon," *Journal of Physics C*, vol. 12, no. 13, pp. 2497–2508, 1979.
- [12] W. Hehre, L. Radom, P. Schleyer, and J. Pople, *Ab Initio Molecular Orbital Theory*, Wiley, New York, NY, USA, 1986.
- [13] W. J. Hehre, R. F. Stewart, and J. A. Pople, "Self-consistent molecular-orbital methods. I. Use of gaussian expansions of slater-type atomic orbitals," *The Journal of Chemical Physics*, vol. 51, no. 6, pp. 2657–2664, 1969.
- [14] J. B. Collins, P. V. R. Von Schleyer, J. S. Binkley, and J. A. Pople, "Self-consistent molecular orbital methods. XVII. Geometries and binding energies of second-row molecules. A comparison of three basis sets," *The Journal of Chemical Physics*, vol. 64, no. 12, pp. 5142–5151, 1976.
- [15] A. M. Dobrotvorskii and E. A. Evarestov, "The quasi-molecular large unit cell model in the theory of deep levels in imperfect crystals: point defects in graphitic boron nitride," *Physica Status Solidi B*, vol. 66, no. 1, pp. 83–91, 1974.
- [16] M. A. Abdulsattar, "Size effects of semiempirical large unit cell method in comparison with nanoclusters properties of diamond-structured covalent semiconductors," *Physica E*, vol. 41, no. 9, pp. 1679–1688, 2009.
- [17] M. J. Frisch, G. W. Trucks, H. B. Schlegel et al., *Gaussian 03, Revision B.01*, Gaussian, Pittsburgh, Pa, USA, 2003.
- [18] C. Kittel, *Introduction to Solid State Physics*, John Wiley & Sons, New York, NY, USA, 5th edition, 1976.
- [19] S. Froyen and M. L. Cohen, "Structural properties of III–V zinc-blende semiconductors under pressure," *Physical Review B*, vol. 28, no. 6, pp. 3258–3265, 1983.
- [20] R. Ahmed, F. Aleem, S. J. Hashemifar, and H. Akbarzadeh, "First-principles study of the structural and electronic properties of III-phosphides," *Physica B*, vol. 403, no. 10–11, pp. 1876–1881, 2008.
- [21] F. D. Murnghan, "The compressibility of media under extreme pressures," *Proceedings of the National Academy of Sciences of The United States of America*, vol. 30, no. 9, pp. 244–247, 1944.
- [22] W. Martienssen and H. Warlimont, Eds., *Springer Handbook of Condensed Matter and Materials Data*, Springer, Berlin, Germany, 2005.
- [23] N. A. Nama, M. A. Abdulsattar, and A. M. Abdul-Lettif, "Surface and core electronic structure of oxidized silicon nanocrystals," *Journal of Nanomaterials*, vol. 2010, Article ID 952172, 2010.
- [24] N. H. Aysa, M. A. Abdulsattar, and A. M. Abdul-Lettif, "Electronic structure of germanium nanocrystals core and (001)-(1×1) oxidised surface," *Micro & Nano Letters*, vol. 6, no. 3, pp. 137–140, 2011.
- [25] H. C. Casey Jr. and M. B. Panish, *Heterostructure Lasers, Part A, Fundamental Principles and Part B, Materials and Operating Characteristics*, Academic Press, New York, NY, USA, 1978.
- [26] M. Shishkin and G. Kresse, "Self-consistent GW calculations for semiconductors and insulators," *Physical Review B*, vol. 75, no. 23, Article ID 235102, 2007.
- [27] M. A. Abdulsattar, "Mesoscopic fluctuations of electronic structure properties of boron phosphide nanocrystals," *Electronic Materials Letters*, vol. 6, no. 3, pp. 97–101, 2010.
- [28] T. Shimazaki and Y. Asai, "Energy band structure calculations based on screened Hartree-Fock exchange method: Si, AlP, AlAs, GaP, and GaAs," *Journal of Chemical Physics*, vol. 132, no. 22, Article ID 224105, 2010.
- [29] M. Causa and A. Zupan, "Density functional LCAO calculation of periodic systems. A posteriori correction of the Hartree-Fock energy of covalent and ionic crystals," *Chemical Physics Letters*, vol. 220, no. 3–5, pp. 145–153, 1994.
- [30] S. Lee, J. Kang, and M. Kang, "Structural properties of semiconductors in the generalized gradient approximation," *Journal of the Korean Physical Society*, vol. 31, no. 5, pp. 811–814, 1997.
- [31] S. J. Sque, R. Jones, and P. R. Briddon, "Structure, electronics, and interaction of hydrogen and oxygen on diamond surfaces," *Physical Review B*, vol. 73, no. 8, Article ID 085313, pp. 1–15, 2006.
- [32] H.M. Abduljalil, M.A. Abdulsattar, and S.R. Al-Mansoury, "SiGe nanocrystals core and surface electronic structure from Ab initio large unit cell calculations," *Micro & Nano Letters*, vol. 6, no. 6, pp. 386–389, 2011.
- [33] M. A. Abdulsattar, "Ab initio large unit cell calculations of the electronic structure of diamond nanocrystals," *Solid State Sciences*, vol. 13, no. 5, pp. 843–849, 2011.
- [34] I. V. Kityk, A. Kassiba, K. Plucinski, and J. Berdowski, "Band structure of large-sized SiC nanocomposites," *Physics Letters A*, vol. 265, no. 5–6, pp. 403–410, 2000.



Hindawi

Submit your manuscripts at
<http://www.hindawi.com>

